Supporting Information: Multimedia Modeling of Engineered Nanoparticles with SimpleBox4nano: Model Definition and Evaluation

Johannes A.J. Meesters[*†], Albert. A. Koelmans[‡,§], Joris T.K. Quik[‡], A. Jan Hendriks[†], Dik van de Meent[†]*

† Radboud University Nijmegen, Institute for Water and Wetland Research, Department of Environmental Science, P.O. Box 9010, NL - 6500 GL Nijmegen, The Netherlands, ‡ Aquatic Ecology and Water Quality Management Group, Department of Environmental Sciences, Wageningen University, P.O. Box 47, 6700 AA Wageningen, The Netherlands, § IMARES – Institute for Marine Resources & Ecosystem Studies, Wageningen UR, P.O. Box 68, 1970 AB IJmuiden, The Netherlands

* Corresponding author: Phone: +31-(0)24-3652393; Fax: + 31 (0)24 355 34 50; e-mail: j.meesters@science.ru.nl

Keywords: Multimedia Modeling Environmental Concentrations Engineered Nanoparticles

Table of Contents

Mass balance equations expressed as matrix algebra: S17

Author information: S35

References used for supporting information: S35-S40

Table S1. Glossary of terms: S5-S16

Table S2. First-order rate constants for total removal per compartment and species of ENP: S18

Table S3. Derivation of aggregation and attachment rates for compartments atmosphere, water, soil and sediment: S19

Table S4. Deriving coagulation rates between ENPs and natural aerosol particles: S20

Table S5. Characterization of background concentrations of natural aerosol particles: S20

Table S6. Collision rates between ENPs with natural colloids and larger suspended particles in water: S21

Table S7. Experimentally derived efficiencies for hetero-aggregation between ENPs and natural colloidal particles in different water types: S21

Table S8. Electrophoretic mobility given for different ENPs in different water types: S23

Table S9. Theoretical derivation of aggregation efficiencies between ENPs and natural colloids: S24

Table S10. Experimentally derived efficiencies for attachment of ENPs to suspended particulates in different water types: S25

Table S11. Theoretical derivation of attachment efficiencies between ENPs and suspended particles in surface waters: S25

Table S12. Application of the particle filtration theory: S26

Table S13. Experimentally derived attachment efficiencies between engineered Cu^0 nanoparticles and the solid grains of a saturated quartz column: S27

Table S14. Theoretical derivation of attachment efficiencies between ENPs and the solid grains in porous media using the interaction force boundary layer approximation: S28

Table S15. Characterization of size and mass of altered species of ENPs: S28

Table S16. Scavenging coefficients as function of particle size and density: S29

Table S17. Dry deposition velocities as a function of particle size and density: S30

Table S18. ENP dissolution rates for different mechanisms: S31

Table S19. First-order rate constants for advective transports: S31

Table S20. System dimensions for realistic nano-TiO_2 emission scenario in Switzerland: S32

Table S21. Input parameter and their values for the realistic nano-TiO_2 emission scenario in Switzerland: S32

Table S22.The first-order rate constant values that SimpleBox4nano calculates for environmental transport and removal processes for the Mueller and Nowack nano-TiO_2 emission scenario: S33-S35

Figure S1. Aggregation efficiency as a function of electrophoretic mobility: S22

Table S1. Glossary of terms

Symbol	Description	Value / Unit	Eq. Nr.	Ref.
A	First-order removal and transport rate constant matrix	s^{-1}	1	1
A_{ENP}	ENP surface	m^2	-	(-)
$A_{Hamaker(123)}$	Overall Hamaker constant for ENP (1), water (2), and grain collector (3)	(-)	-	2
$A_{Arrhenius}$	Arrhenius constant for Arrhenius equations	(-)	-	3
A_s	Analytical Smoluchowski-Levich solution	(-)	35	4
$á_{veg}$	Vegetation hair width	$1.0 .10^{-5}$ m	-	5
$Á_{veg}$	Vegetation large collection radii	$5.0 .10^{-4}$ m	-	5
$c_{env.cond}$	Influence on dissolution rate by environmental conditions	(-)	-	3
C_0	Experiment's initial concentration	$N.m^{-3}$	-	1
Cc_i	Cunningham coefficient for atmospheric particle *i*	(-)	13	6
$\bar{c}_{thermal(i)}$	Thermal velocity of particle *i* in air	$m.s^{-1}$	15	7
$C_{(t)}$	Experiment's concentration at time *t*	$N.m^{-3}$	-	1
C_v/C_d	Viscous versus total drag ratio	0.3	-	5
d_{Grain}	Grain collector diameter	0.256 mm	-	8

$D_{air(i)}$	Diffusivity of particle *i* in air	$m^2.s^{-1}$	12	9
D_i	Diffusivity of particle *i* in water	$m^2.s^{-1}$	41	10
D_{SP}	Diffusivity of solution product	$m^2.s^{-1}$	-	(-)
d_{ENP}	Diameter of the engineered nanoparticle	m	-	(-)
d_{rain}	Representative diameter of a rain droplet	m	MA7*[1]	11,12
e	Emission of ENPs to the environment	$g.s^{-1}$	1	1
$e_{electron}$	Elemental charge	$1.6\ 10^{-19}$ V	-	(-)
$E_{\Lambda i}$	Total raindrop collection efficiency for atmospheric particle *i*	(-)	52	13
$E_{\Lambda Brown}$	Raindrop collection efficiency for Brownian motion	(-)	53	13
$E_{\Lambda intercept}$	Raindrop collection efficiency for interception	(-)	54	13
$E_{\Lambda grav}$	Raindrop collection efficiency for gravitational impaction	(-)	55	13
$E_{dBrown(soil)}$	Collection efficiency of Brownian motion to soil surfaces	(-)	67	5
$E_{dBrown(water)}$	Collection efficiency of Brownian motion to surface water	(-)	64	5
$E_{d\ int.cept(soil)}$	Collection efficiency of interception to soil	(-)	68	5
$E_{d\ int.cept\ (water}$	Collection efficiency of interception to surface water	(-)	65	5
$E_{dgrav(soil)}$	Collection efficiency of inertial impaction to soil	(-)	69	5
$E_{dgrav(water)}$	Collection efficiency of inertial impaction to surface water	(-)	66	5

$E_{activation}$	Required activation energy for dissolution	J	-	3
f	Porous medium porosity	(-)	0.456	14-16
$f_{coag(i,j)}$	Polydisperse coagulation coefficient between atmospheric particle *i* and *j*.	s^{-1}	10	9
$f_{col(i,j)}$	Collision rate between ENPs and natural particles in aqueous media	s^{-1}	20	17
f_{Brown}	Collision frequency due to Brownian motion	s^{-1}	16	17
$f_{Intercept}$	Collision frequency due to interception	s^{-1}	17	17
f_{grav}	Collision frequency due to gravitational settling differences	s^{-1}	18	17
fr_{iv}	Fraction of interception by vegetation	0.01	-	5
$f_{Brenner(0,0,r/r+h)}$	Brenner function for deposition to surfaces	(-)	45	18
$g_{1(H)}$	Universal hydrodynamic function	(-)	45	2
G_{shear}	Surface water shear rate	10 s^{-1}	-	17
h	Separation distance between particle *i* and *j*	m	-	(-)
I	Ionic strength of the aqueous medium	1-10 $.10^{-3}$ M	-	19
k_b	Boltzmann constant	1.38 $.10^{-23}$ $J.K^{-1}$	-	(-)
$k_{\Lambda ARagg}$	Rain drop collection rate for aggregated ENP species	s^{-1}	51	(-)
$k_{\Lambda ARatt}$	Rain drop collection rate for attached ENP species	s^{-1}	51	(-)

$k_{\Lambda AR free}$	Rain drop collection rate for free ENP species	s^{-1}	51	(-)
k_{aggA}	Aggregation rate for ENPs with aerosol particles in dry air (A)	s^{-1}	2	(-)
k_{aggS}	Aggregation rate for ENPs with natural colloids in soil (S) pore water	s^{-1}	6	(-)
k_{aggSE}	Aggregation rate for ENPs with natural colloids in sediment (SE) pore water	s^{-1}	8	(-)
k_{aggW}	Aggregation rate for ENPs with natural colloids in surface water (W)	s^{-1}	4	(-)
k_{attA}	Attachment rate for ENPs with coarse particles in dry air (A)	s^{-1}	3	(-)
k_{attS}	Attachment rate for ENPs with solid grains in soil (S)	s^{-1}	7	(-)
k_{attSE}	Attachment rate for ENPs with solid grains in sediment (SE)	s^{-1}	9	(-)
k_{attW}	Attachment rate for ENPs with suspended particles in surface water (W)	s^{-1}	5	(-)
k_{bur}	Burial of ENPs to deeper sediments	s^{-1}	76	14-16
$k_{depASagg}$	First-order rate constant for dry deposition from dry air (A) to soil (S) for aggregated ENP species	s^{-1}	MA 6*[1]	(-)
$k_{depASatt}$	First-order rate constant for dry deposition from dry air (A) to soil (S) for attached ENP species	s^{-1}	MA 6*[1]	(-)
$k_{depASfree}$	First-order rate constant for dry deposition from dry air (A) to soil (S) for free ENP species	s^{-1}	MA 6*[1]	(-)

$k_{depAWagg}$	First-order rate constant for dry deposition from dry air (A) to water (W) for aggregated ENP species	s^{-1}	MA 6*[1]	(-)
$k_{depAWatt}$	First-order rate constant for dry deposition from dry air (A) to soil (W) for attached ENP species	s^{-1}	MA 6*[1]	(-)
$k_{depAWfree}$	First-order rate constant for dry deposition from dry air (A) to soil (W) for free ENP species	s^{-1}	MA 6*[1]	(-)
$k_{depRSagg}$	First-order rate constant for wet deposition from rain (R) to soil (S) for aggregated ENP species	s^{-1}	MA 6*[1]	(-)
$k_{depRSatt}$	First-order rate constant for wet deposition from rain (R) to soil (S) for attached ENP species	s^{-1}	MA 6*[1]	(-)
$k_{depRSfree}$	First-order rate constant for wet deposition from rain (R) to soil (S) for free ENP species	s^{-1}	MA 6*[1]	(-)
$k_{depRWagg}$	First-order rate constant for wet deposition from rain (R) to water (W) for aggregated ENP species	s^{-1}	MA 6*[1]	(-)
$k_{depRWatt}$	First-order rate constant for wet deposition from rain (R) to soil (W) for attached ENP species	s^{-1}	MA 6*[1]	(-)
$k_{depRWfree}$	First-order rate constant for wet deposition from rain (R) to soil (W) for free ENP species	s^{-1}	MA 6*[1]	(-)
$k_{depWSEagg}$	First-order rate constant for deposition from water (W) to sediments (SE) for aggregated ENP species	s^{-1}	MA 6*[1]	(-)
$k_{depWSEatt}$	First-order rate constant for deposition from water (W) to sediments (SE) for attached ENP species	s^{-1}	MA 6*[1]	(-)

$k_{depWSEfree}$	First-order rate constant for deposition from water (W) to sediments (SE) for free ENP species	s^{-1}	MA 6*[1]	(-)
$k_{erosionSWatt}$	First-order rate constant for run-off from soil (S) to water (W) for attached ENP species	s^{-1}	74	(-)
$k_{rsSEWagg}$	First-order rate constant for resuspension from sediments (SE) to water (W) for aggregated ENP species	s^{-1}	69	14-16
$k_{rsSEWatt}$	First-order rate constant for resuspension from sediments (SE) to water (W) for attached ENP species	s^{-1}	70	14-16
$k_{rsSEWfree}$	First-order rate constant for resuspension from sediments (SE) to water (W) for free ENP species	s^{-1}	69	14-16
$k_{runSWagg}$	First-order rate constant for run-off from soil (S) to water (W) for aggregated ENP species	s^{-1}	73	(-)
$k_{runSWfree}$	First-order rate constant for run-off from soil (S) to water (W) for free ENP species	s^{-1}	73	(-)
Kn_i	Knudsen number of the atmospheric particle *i*	(-)	14	6
K_F	Pseudo-first-order rate constant for attachment efficiency	s^{-1}	44	2
m	Steady state ENP mass per compartment and species	g	1	1
m_{as}	Mass of altered species particle	g	47	(-)
mCP	Mass of counter particle	g	-	(-)
m_i	Individual mass particle *i*	g	-	(-)
m_{ENP}	Mass of the engineered nanoparticle	g	-	(-)

M_{SP}	Molarity of solution product	M	-	(-)
N_A	Avogadro's number	6.02 x 10^{-23} mol^{-1}	-	(-)
N_{acc}	Number concentration of Aitken accumulation mode aerosol particles	2.9 10^9 $N.m^{-3}$	-	20
N_{coarse}	Number concentration of coarse mode aerosol particles	3 10^5 $N.m^{-3}$	-	20
$N_{NC(S)}$	Number concentration of natural colloids in soil pore water	1 . 10^{11} $N.m^{-3}$	-	21
$N_{NC(SE)}$	Number concentration of natural colloids in sediment pore water	1 . 10^{11} $N.m^{-3}$	-	21
$N_{NC(W)}$	Number concentration of natural colloids in surface water	1 . 10^{11} $N.m^{-3}$	-	21
N_{nuc}	Number concentration of nucleation mode aerosol particles	3.2 10^9 $N.m^{-3}$	-	20
$N_{SP(W)}$	Number concentration of suspended particles (>450 nm) in surface water	$N.m^{-3}$	-	21
N_R	Aspect ratio number	(-)	37	4
N_{PE}	Peclet Number	(-)	38	4
N_{VDW}	Van der Waals attraction number	(-)	39	4
N_G	Gravity number	(-)	40	4
p_0	Precipitation rate	2.22 10-8 $m.s^{-1}$	-	14-16
r	Radius	m	-	(-)

r_{NC}	Radius of natural colloids in water	300 nm	-	21
r_{NLP}	Radius of natural larger particles in water	$2.8\ 10^{5}$	-	14-16
r_{as}	Radius of individual altered species particle	m	50	(-)
R	Ideal gas constant	8.314 $J.K^{-1}.mol^{-1}$	-	(-)
R_A	Aerodynamic resistance	33 $s.m^{-1}$; 333 $s.m^{-1}$	-	5
r_{rain}	Rain drop radius	m	MA 7[*1]	11,12
$R_{S(i)}$	Surface resistance for atmospheric particle *i*	$s.m^{-1}$	-	5
Re	Reynolds number	(-)	56	13
S(β)	Function of Spielman & Friedlander for surface collisions	(-)	-	22
Sc_i	Schmidt number of atmospheric particle *i*	(-)	-	13
$[SP_{aq(0-\delta D)}]$	Solution product concentration within diffusion boundary layer	$mg.l^{-1}$		(-)
$[SP_{bg}]$	Background concentration of solution product	$mg.l^{-1}$	-	(-)
St*	Critical Stokes Number	(-)	61	13
St_i	Stokes number of atmospheric particle *i*	(-)	59	13
t	Time	s	-	(-)
T	Temperature	K	-	(-)

T_{air}	Air temperature	285 K	-	23
u_*	Friction velocity	0.19 $m.s^{-1}$	-	23
U_{Darcy}	Darcy approach velocity	9 $10^{-6} m.s^{-1}$	-	4
$v_{dep(i)}$	Dry deposition velocity atmospheric particle *i*	$m.s^{-1}$	62	5
$v_{set(i)}$	Gravitational settling velocity of suspended particle *i*	$m.s^{-1}$	19	24
$v_{term(i)}$	Terminal velocity of atmospheric particle *i*	$m.s^{-1}$	57	13
$v_{term(rain)}$	Representative terminal velocity of a rain droplet	$m.s^{-1}$	57	13
V_{CP}	Volume of individual counter particle	m^3	-	(-)
V_{ENP}	Volume of individual ENP	m^3	-	(-)
V_{as}	Volume of individual altered species particle	m^3	48	(-)
$V_{EDL(i,j)}$	Electric double layer repulsive energy between particle *i* and *j*	J	26, 30	2
$V_{max(i,j)}$	Maximum interaction energy barrier between particle *i* and *j*	J	24	2
$V_{VDW(i,j)}$	Van der Waals attractive energy between particle *i* and *j*	J	25, 29	2
V_T	Total energy barrier between particle *i* an *j*	J	46	2
z	Counter ion valence	e.g. 4	-	(-)
α_{agg}	Aggregation efficiency between ENP and natural colloid (<450 nm)	(-)	22	2
α_{att}	Attachment efficiency between ENP and large particle (>450	(-)	28, 41	2

	nm)			
α_{Cc}	Empirical constant for deriving Cunningham coefficient	1.142	-	6
β_{Cc}	Empirical constant for deriving Cunningham coefficient	0.558	-	6
β_{IFBL}	Interaction force boundary layer approximation parameter	(-)	43	2
$\beta_{i,j}$	Transitional correction coefficient for coagulation between atmospheric particle *i* and *j*.	(-)	11	9
γ_{Cc}	Empirical constant for deriving Cunningham coefficient	0.999	-	6
γ_s	Porosity dependency parameter	(-)	36	4
ψ_i	Surface potential of particle *i*	V	-	(-)
ψ_{NP}	Surface potential of natural particle	55 mV	-	25
ε_0	Dielectric permittivity in vacuum	8.854×10^{-12} $F.m^{-1}$	-	(-)
ε_r	Relative dielectric permittivity of water	78.5 at 25˚C	-	(-)
η_0	Total collection efficiency for deposition of ENPs onto solid grains in porous media	(-)	32	4
η_{Brown}	Collection efficiency for deposition onto solid grains by Brownian motion	(-)	33	4
$\eta_{Intercept}$	Collection efficiency for deposition onto solid grains by interception	(-)	34	4
ηg_{rav}	Collection efficiency for deposition onto solid grains by	(-)	35	4

	gravitational impaction			
η_{air}	Kinematic viscosity of air	$1{,}48.10^{-5}$ $J.m^{-3}.s^{-1}$	-	(-)
κ_{Debye}	Debye length	m	-	26
λ_{air}	Mean free path in air	66.10^{-9} m	-	27
λ_{cw}	Characteristic wave length	≈100 nm	-	28
λ_{filter}	Filtration in porous media	m^{-1}	31	4
Λ_i	Scavenging coefficient of atmospheric particle *i*	s^{-1}	51	13
Γ_i	Dimensionless surface potential of particle *i*	(-)	27	2
ρ_{as}	Density of individual altered species particle	$kg.m^{-3}$	49	(-)
$\rho_{aerosol}$	Assumed density for nucleation, accumulation and coarse mode aerosols	$1.371 .10^{5}$ $g.m^{-3}$	-	29
ρ_{air}	Density of air	1.225 $kg.m^{-3}$	-	(-)
ρ_{ENP}	Density of ENP	$kg.m^{-3}$	-	(-)
ρ_i	Density of particle *i*	$kg.m^{-3}$	-	(-)
ρ_{water}	Density of water	998 $kg.m^{-3}$	-	(-)
δ_D	Diffusion boundary layer thickness	m	23	26

$\tau_{air(i)}$	Relaxation of atmospheric particle *i* in air	s	60	13
μ_{air}	Dynamic viscosity of air	$1.81\ 10^{-5}$ $J.m^{-3}.s^{-1}$	-	(-)
μ_{water}	Dynamic viscosity of water	8.9×10^{-4} Pa.s	-	(-)

*1 MA= Main Article

Mass balance equations expressed as matrix algebra

$$m = -A^{-1} \cdot e \qquad \text{(Eq. S1)}$$

The mass balance equations of SB4N, with m is steady state ENP mass (g) per compartment and species, emission e to the environment ($g.s^{-1}$) and transport and removal rates (s^{-1}) expressed in matrix *A*

$$m = \begin{bmatrix} m_{Afree} \\ m_{Aagg} \\ m_{Aatt} \\ m_{Rfree} \\ m_{Ragg} \\ m_{Ratt} \\ m_{Sfree} \\ m_{Sagg} \\ m_{Satt} \\ m_{Wfree} \\ m_{Wagg} \\ m_{Watt} \\ m_{SEfree} \\ m_{SEagg} \\ m_{SEatt} \end{bmatrix}, = \begin{bmatrix} e_{Afree} \\ 0 \\ 0 \\ 0 \\ 0 \\ 0 \\ e_{Sfree} \\ 0 \\ 0 \\ e_{Wfree} \\ 0 \\ 0 \\ 0 \\ 0 \\ 0 \end{bmatrix}, \text{and}$$

$$A = \begin{bmatrix} -(\Sigma k_{rAfree}) & 0 & 0 & 0 & 0 & 0 & 0 & 0 & 0 & 0 & 0 & 0 & 0 & 0 & 0 \\ k_{aggA} & -(\Sigma k_{rAagg}) & 0 & 0 & 0 & 0 & 0 & 0 & 0 & 0 & 0 & 0 & 0 & 0 & 0 \\ k_{attA} & 0 & -(\Sigma k_{rAatt}) & 0 & 0 & 0 & 0 & 0 & 0 & 0 & 0 & 0 & 0 & 0 & 0 \\ k_{\Lambda\Lambda Rfree} & 0 & 0 & -(\Sigma k_{rRfree}) & 0 & 0 & 0 & 0 & 0 & 0 & 0 & 0 & 0 & 0 & 0 \\ 0 & k_{\Lambda\Lambda Ragg} & 0 & 0 & -(\Sigma k_{rRagg} & 0 & 0 & 0 & 0 & 0 & 0 & 0 & 0 & 0 & 0 \\ 0 & 0 & k_{\Lambda att} & 0 & 0 & -(\Sigma k_{rRatt}) & 0 & 0 & 0 & 0 & 0 & 0 & 0 & 0 & 0 \\ k_{depASfree} & 0 & 0 & k_{depRSfree} & 0 & 0 & -(\Sigma k_{rSfree}) & 0 & 0 & 0 & 0 & 0 & 0 & 0 & 0 \\ 0 & k_{depASagg} & 0 & 0 & k_{depRSagg} & 0 & k_{aggS} & -(\Sigma k_{rSagg}) & 0 & 0 & 0 & 0 & 0 & 0 & 0 \\ 0 & 0 & k_{depASatt} & 0 & 0 & k_{depRSatt} & k_{attS} & 0 & -(\Sigma k_{rSatt}) & 0 & 0 & 0 & 0 & 0 & 0 \\ k_{depAWfree} & 0 & 0 & k_{depRWfree} & 0 & 0 & k_{runSWfree} & 0 & 0 & -(\Sigma k_{rWfree}) & 0 & 0 & k_{rsSEWfree} & 0 & 0 \\ 0 & k_{depAWagg} & 0 & 0 & k_{depRWagg} & 0 & 0 & k_{runSWagg} & 0 & k_{aggW} & -(\Sigma k_{rWagg}) & 0 & 0 & k_{rsSEWagg} & 0 \\ 0 & 0 & k_{depAWatt} & 0 & 0 & k_{depRWatt} & 0 & 0 & k_{erosionSWatt} & k_{attW} & 0 & -(\Sigma k_{rWatt}) & 0 & 0 & k_{rsSEWatt} \\ 0 & 0 & 0 & 0 & 0 & 0 & 0 & 0 & 0 & k_{depWSEfree} & 0 & 0 & -(\Sigma k_{rSEfree} & 0 & 0 \\ 0 & 0 & 0 & 0 & 0 & 0 & 0 & 0 & 0 & 0 & k_{depWSEagg} & 0 & k_{aggSE} & -(\Sigma k_{rSEagg}) & 0 \\ 0 & 0 & 0 & 0 & 0 & 0 & 0 & 0 & 0 & 0 & 0 & k_{depWSEatt} & k_{attSE} & 0 & -(\Sigma k_{rSEatt} \end{bmatrix}$$

Table S2. First-order rate constants for total removal (Σk_r) per compartment and species of ENP

Species in compartment	Total sum of removal rates per species in compartment
Free in dry air:	$\Sigma k_{rAfree} = k_{aggA} + k_{attA} + k_{\Lambda ARfree} + k_{depASfree} + k_{depAWfree}$
Agg. in dry air:	$\Sigma k_{rAagg} = k_{\Lambda ARagg} + k_{depASagg} + k_{depAWagg}$
Att. in dry air:	$\Sigma k_{rAatt} = k_{\Lambda ARatt} + k_{depASatt} + k_{depAWatt}$
Free in rain:	$\Sigma k_{rRfree} = k_{depRSfree} + k_{depRWfree} + k_{dissolveRfree}$
Agg. in rain:	$\Sigma k_{rRagg} = k_{depRSagg} + k_{depRWagg} + k_{dissolveRagg}$
Att. in rain:	$\Sigma k_{rRatt} = k_{depRSatt} + k_{depRWatt} + k_{dissolveRatt}$
Free in soil pore water:	$\Sigma k_{rSfree} = k_{aggS} + k_{attS} + k_{leachSfree} + k_{runSWfree} + k_{dissolveSfree}$
Agg. in soil pore water:	$\Sigma k_{rSagg} = k_{leachSagg} + k_{runSWagg} + k_{dissolveSagg}$
Att. to soil grains:	$\Sigma k_{rSatt} = k_{erosionSWatt} + k_{dissolveSatt}$
Free in water:	$\Sigma k_{rWfree} = k_{aggW} + k_{attW} + k_{depWSEfree} + k_{dissolveWfree}$
Agg. in water:	$\Sigma k_{rWagg} = k_{depWSEagg} + k_{dissolveWagg}$
Att. in water:	$\Sigma k_{rWatt} = k_{depWSEatt} + k_{dissolveWatt}$
Free in sediment pore water:	$\Sigma k_{rSEfree} = k_{aggSE} + k_{attSE} + k_{burSEfree} + k_{rsSEWfree} + k_{dissolveSEfree}$
Agg. in sediment pore water:	$\Sigma k_{rSEagg} = k_{burSEagg} + k_{rsSEWagg} + k_{dissolveSEagg}$
Att. to sediment grains:	$\Sigma k_{rSEatt} = k_{burSEatt} + k_{rsSEWatt} + k_{dissolveSEatt}$

Table S3. Derivation of aggregation and attachment rates for compartments atmosphere (A), water (W), soil (S) and sediment (SE)

Compartment	Equations for attachment and aggregation rate	
Atmosphere	2	$k_{aggA} = f_{coag(ENP,nuc)} \cdot \alpha_{ENP,nuc} \cdot N_{nuc} + f_{coag(ENP,acc)} \cdot \alpha_{ENP,acc} \cdot N_{acc}$
	3	$k_{attA} = f_{coag(ENP,coarse)} \cdot \alpha_{ENP,coarse} \cdot N_{coarse}$
Surface water	4	$k_{agg(W} = f_{col(ENP,NC)} \cdot \alpha_{agg(ENP,NC)} \cdot N_{NC(W)}$
	5	$k_{attW} = f_{col(ENP,NLP)} \cdot \alpha_{att(ENP,SP)} \cdot N_{SP(W)}$
Soil	6	$k_{aggS} = f_{col(ENP,NC)} \cdot \alpha_{agg(ENP,NC)} \cdot N_{NC(S)}$
	7	$k_{attS} = \lambda_{filter} \cdot \alpha_{att(ENP,grain)} \cdot \eta_{0(ENP,grain)} \cdot U_{Darcy}$
Sediment	8	$k_{aggSE} = f_{col(ENP,NC)} \cdot \alpha_{agg(ENP,NC)} \cdot N_{NC(SE)}$
	9	$k_{attSE} = \lambda_{filter} \cdot \alpha_{att(ENP,grain)} \cdot \eta_{0(ENP,grain)} \cdot U_{Darcy}$

Table S4. Deriving coagulation rates between ENPs and natural aerosol particles[7,9]

Parameter	Equation	
Coagulation coefficient	10	$f_{coag(i,j)} = 4\pi\left(r_i + r_j\right)\left(D_{air(i)} + D_{air(j)}\right)$
Transitional correction coefficient	11	$\alpha_{(i,j)} = \left(1 + \frac{4\left(D_{air(i)} + D_{air(j)}\right)}{(r_i + r_j)\sqrt{\bar{c}_{thermal(i)}{}^2 + \bar{c}_{thermal(j)}{}^2}}\right)^{-1}$
Particle diffusivity in air	12	$D_{air(i)} = (k_b T_{air} Cc_i)/(6\pi\eta_{air} r_i)$
Particle Cunningham coefficient	13	$Cc_i = 1 + Kn_i(\alpha_{Cc} + \beta_{Cc} \cdot e^{-\frac{\gamma_{Cc}}{Kn_i}})$
Particle Knudsen number	14	$Kn_i = \lambda_{air}/r_i$
Particle thermal velocity	15	$\bar{c}_{thermal(i)} = (8k_b T_{air})/\sqrt{\pi m_i}$

Table S5. Characterization of background concentrations of natural aerosol particles*[1 20]

Mode	Diameter (nm)	Size standard deviation	Number concentration ($N.m^{-3}$)
Nucleation	20	0.245	$3.2\ 10^9$
Accumulation	116	0.217	$2.9\ 10^9$
Coarse	1800	0.380	$3\ 10^5$

*1. The density of an aerosol particle itself is characterized as $1.37\ 10^2$ $kg.m^{-3}$ based on the average chemical composition of measured aerosols[29]

Table S6. Collision rates between ENPs with natural colloids (<450 nm) and larger suspended particles in water.[30]

Collision mechanism	Equation	
Brownian motion	16	$f_{Brown(i,j)} = \frac{2k_bT}{3\mu_{water}} \frac{\left(r_i + r_j\right)^2}{r_i \cdot r_j}$
Interception	17	$f_{Intercept(i,j)} = \frac{4}{3} G_{shear} \left(r_i + r_j\right)^3$
Differential settling	18	$f_{grav(i,j)} = \pi \left(r_i + r_j\right)^2 \cdot \left\lvert v_{set(i)} - v_{set(j)} \right\rvert$
Gravitational settling velocity	19	$v_{set(i)} = \frac{2\left(\rho_i - \rho_{water}\right) g\, {r_i}^2}{9\mu_{water}}$
Total collision frequency coefficient	20	$f_{col(i,j)} = f_{Brown(i,j)} + f_{Intercept(i,j)} + f_{grav(i,j)}$
Collision rate	21	$k_{col(i,j)} = f_{col(i,j)} \cdot N_j$

Table S7. Experimentally derived efficiencies for hetero-aggregation (α_{agg})between ENPs and natural colloidal particles in different water types. Original data from Quik, J.T.K., Ph.D. Dissertation, Radboud University Nijmegen, The Netherlands, 2013.[31]

		Aggregation efficiencies (α_{agg})			
Sample Site (The Netherlands)	Water type	Nano-C60	Nano-CeO2	Nano-SiO2-Ag	Nano-PVP-Ag
Karregat	Pool	n.a.	0.161	n.a.	0.692
Brabantse Aa	Brook	6.75E-03	n.a.	0.222	n.a.
River Rhine	River	n.a.	0.996	0.444	0.292
IJsselmeer	Lake	n.a.	0.121	0.252	0.102
Nieuwe Waterweg	Canal	0.231	0.854	0.603	0.678
North Sea	Sea	1	1	1	1

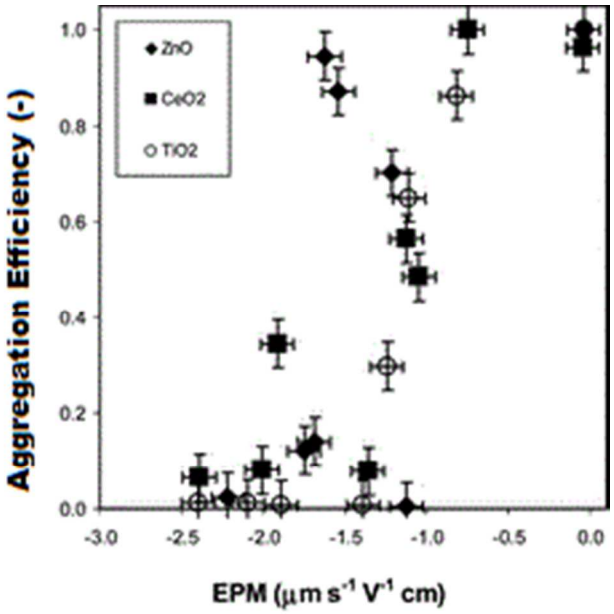

Figure S1. Aggregation efficiency as a function of electrophoretic mobility (EPM).Original data from Keller et al., 2010. Environmental Science & Technology, **2010**, *44*, 1962-1967.[32]

Table. S8 Electrophoretic mobility (EPM) in $\mu ms^{-1}V^{-1}cm$ given for different ENPs in different water types. Original data from Keller et al., 2010. Environmental Science & Technology, **2010**, *44*, 1962-1967. [32]

Water Type	nano-TiO2	nano-CeO2	nano-ZnO
Natural Seawater	-0.04±0.09	-0.05±0.24	-0.04±0.26
Artificial Seawater	-0.05±0.15	-0.04±0.09	-0.27±0.52
Lagoon	-0.82±0.09	-0.75±0.16	-1.54±0.17
Groundwater	-1.11±0.03	-1.05±0.05	-1.21±0.03
River	-1.24±0.13	-1.13±0.11	-1.63±0.07
Treated Effluent	-1.39±0.05	-1.36±0.05	-1.13±0.04
Mesocosm Effluent	-1.89±0.04	-1.91±0.05	-1.75±0.04
Storm Water	-2.09±0.05	-2.01±0.05	-1.69±0.07
Mesocosm freshwater	-2.4±0.05	-2.39±0.09	-2.22±0.06

Table S9. Theoretical derivation of aggregation efficiencies between ENPs and natural colloids*[1 2]

Parameter	Equation	
Aggregation efficiency	22	$\alpha_{agg} \approx \kappa_{Debye} 2r_i e^{\left(-\frac{V_{max(i,j)}}{k_b T}\right)}$
Diffusion boundary layer	23	$\sigma_D = \kappa_{Debye}^{-1} = \left(\sqrt{(\varepsilon_r \varepsilon_0 k_b T)/(2N_A e^2 I)}\right)^{-1}$
Interaction energy	24	$V_{\max(i,j)} = max\left(V_{EDL(h,i,j)} + V_{VDW(h,i,j)}\right)$
Attractive Van der Waals Energy	25	$V_{VDW(h,i,j)} = -\frac{A_{Hamaker(i,water,j)} r_i r_j}{6h(r_i + r_j)(1 + 14\, h/\lambda_{cw})}$
Repulsive Electric Double Layer Energy	26	$V_{EDL(h,i,j)} = 64\pi\varepsilon_o\varepsilon_r \frac{r_i r_j}{r_i + r_j}\left(\frac{k_b T}{z \cdot e_{electron}}\right)^2 \Gamma_i \Gamma_j \exp(-\kappa \cdot h)$
Dimensionless surface potential	27	$\Gamma_i = tanh\left[\frac{z e_{electron} \Psi_{(i)}}{4 k_b T}\right]$

*1 According to the DLVO theory, the interaction energy between suspended colloidal particles can be evaluated as the sum of the attractive van der Waals (V_{VDW}) and the repulsive electrical double-layer (V_{EDL}) energies. The resultant interaction energy (V_T) determines the work that is necessary for the colloids to stick to each other as they must overcome the repulsive energy between them.[33] In case the ENP and natural colloid are of about equal size a simple approximation ($V_T \approx V_{max}$) for the aggregation efficiency for the two colliding colloids can be applied.[34] The aggregation efficiency (α_{agg})is ultimately derived as a function of the ionic strength of the surrounding water (I), the radii (r_{ENP}, r_{NC}), Hamaker constants ($A_{Hamaker(ENP,water,NC)}$), and surface potentials (Ψ_{ENP}, Ψ_{NC}) of the ENPs and the natural colloids (NC).[2]

Table S10. Experimentally derived efficiencies for attachment of ENPs to suspended particulates in different water types(α_{attW}). Original data from Quik, J.T.K., Ph.D. Dissertation, Radboud University Nijmegen, The Netherlands, 2013.[31]

		Attachment Efficiency(α_{attW})		
Sample Site (The Netherlands)	Water type	Nano-CeO2	Nano-SiO2-Ag	Nano-PVP-Ag
River Rhine	River	0.96	0.98	0.82
Nieuwe Waterweg	Canal	1	1	1
North Sea	Sea	0.85	0.93	0.88

Table S11. Theoretical derivation of attachment efficiencies between ENPs and suspended particles (>450 nm) in surface waters *[1]. [35,36]

	Equations	
Attachment efficiency	28	$\alpha_{att(i,j)} = \left(\int_{\infty}^{\delta_D} \left(V_{VDW(i,j)} + V_{EDL(i,j)} \right) d_h / (k_b \cdot T) \right)^{-1}$
Van der Waals energy	29	$V_{VDW} = -\frac{A_{Hamaker(i,water,j)} \cdot r_i}{12h}$
Electric double layer energy	30	$V_{EDL} = 2\pi\varepsilon_o\varepsilon_r\Gamma_i'\Gamma_j' e^{-\kappa h}$

*1 It is assumed that the interaction between ENPs and larger natural particles can be approached as an interaction between a nanoparticle and a surface, because of their relatively large difference in size (<100 nm versus 450 nm).

Table S12. Application of the particle filtration theory[4]

	Equation	
Filtration	31	$\lambda_{filter} = \frac{3}{2}\frac{(1-f)}{d_{grain} \cdot f}$
Total collection efficiency	32	$\eta_{0(i,j)} = \eta_{Brown} + \eta_{Intercept} + \eta_{grav}$
Brownian collection	33	$\eta_{Brown} = 2.4{A_s}^{1/3}{N_R}^{-0.081}{N_{Pe}}^{-0.715}{N_{VDW}}^{0.053}$
Collection by interception	34	$\eta_{Intercept} = 0.55{N_R}^{1.55}{N_{Pe}}^{-0.125}{N_{VDW}}^{0.125}$
Gravitational collection	35	$\eta_{grav} = 0.22{N_R}^{-0.24}{N_G}^{1.11}{N_{VDW}}^{0.053}$
Porosity dependent parameter	36	$A_S = \frac{2(1-\gamma^5)}{2-3\gamma+3\gamma^5-2\gamma^6}$, with $\gamma = (1-f)^{1/3}$
Aspect ratio Number	37	$N_R = \frac{r_i}{r_j}$
Peclet Number	38	$N_{Pe} = \frac{U_{Darcy} \cdot d_j}{D_i}$
Van der Waals Number	39	$N_{VDW} = \frac{A_{Hamaker(i,water,j)}}{k_b \cdot T}$
Gravity Number	40	$N_G = \frac{2{r_i}^2(\rho_i - \rho_{water})g}{9\mu_{water}U_{Darcy}}$
Diffusivity of particle *i* in water	41	$D_i = \frac{k_b T}{6\pi\mu_{water}r_i}$

Table S13. Experimentally derived attachment efficiencies between engineered Cu^0 nanoparticles and the solid grains of a saturated quartz column. Orignal data from Jones & Su, Water Research. 2012, 46, 2445–2456.[8]

Test	Sample Description	Attachment Rate (k_{att}) (s-1)	Attachment Efficiency (α_{att})
1	Deionised water + 1 mM ph7 Trizma	0.00068	0.1146
2	Deionised water + 1 mM ph9.1 Trizma	0.00011	0.0191
3	Deionised I water + 1 mM ph9.1 Trizma	0.00014	0.0237
4	Deionised water + 1 mg/L Humic Acid	0.00059	0.0996
5	Deionised water + 1 mg/L Humic Acid	0.00044	0.073
6	Deionised water + 1 mg/L Humic Acid	0.00048	0.798
7	Deionised water + 5 mg/L Humic Acid	0.00059	0.0987
8	Deionised water + 10 mg/L Humic Acid	0.00036	0.0601
9	Deionised water + 1 mg/L Fulvic Acid	0.00039	0.0645
10	Deionised water + 1 mg/L Fulvic Acid	0.00039	0.0645

Table S14. Theoretical derivation of attachment efficiencies between ENPs and the solid grains in porous media using the interaction force boundary layer (IFBL) approximation*[1] [22,37]

	Equation	
Attachment efficiency	42	$\alpha_{att(i,j)} = \left(\frac{\beta_{IFBL(i,j)}}{1+\beta_{IFBL(i,j)}}\right) S_{\beta(i,j)}$
IFBL function	43	$\beta_{IFBL(i,j)} = \frac{1}{3}(2)^{1/3}\Gamma\left(\frac{1}{3}\right) {A_s}^{-1/3} \left(\frac{D_i}{U_{Darcy} r_j}\right)^{1/3} \left(\frac{K_{F(i,j)} r_j}{D_i}\right)$
uncorrected pseudo-first rate attachment rate constant	44	$K_{F(i,j)} = D_i \left\{ \int_0^{\delta_D} [g_{1(H)} \exp\left(V_{Total(i,j)}/k_b T\right) - 1] dh \right\}^{-1}$
Brenner function	45	$g_{1(H)} = f_{Brenner(0,0,\frac{r}{h+r})}^{-1} = \left(1 + \frac{3}{4}\left(\frac{r_i}{h+r_i}\right) + 0\left[\left(\frac{r_i}{h+r_i}\right)^2\right]\right)^{-1}$
Total interaction energy	46	$V_{Total(h,i,j)} = V_{VDW(h,i,j)} + V_{EDL(h,i,j)}$

*1 With the IFBL approximation, attachment efficiencies can be derived from the radius (r), density (ρ), surface potential (Ψ) and Hamaker constant ($A_{Hamaker(ENP,water,grain)}$) of the ENP, and the radius of the grain (r_{grain}), porosity ($_f$), and Darcy velocity (U_{Darcy}) of the porous medium, see SI Table 8 [2].

Table S15. Characterization of size and mass of altered species of ENPs (aggregated*1 or attached*1)

Altered species property	Equation	
Mass	47	$m_{as} = m_{ENP} + m_{CP}$
Volume	48	$V_{as} = V_{ENP} + V_{CP}$
Density	49	$\rho_{as} = m_{as}/V_{as}$
Radius	50	$r_{as} = (V_{as}/(4/3\pi))^{1/3}$

*1Further characterization of the Hamaker constant and surface potential of the altered species is not necessary.

Table S16. Scavenging coefficients as function of particle size and density[13]

	Equation	
Scavenging coefficient	51	$k_{\Lambda i} = \Lambda_{\mathrm{i}} = \frac{3}{2}\frac{E_{\Lambda i} p_0}{d_{rain}}$
Collection coefficient	52	$E_{\Lambda i} = E_{\Lambda Brown(i)} + E_{\Lambda Intercept(i)} + E_{\Lambda grav(i)}$
Brownian collection	53	$E_{\Lambda Brown)i)} = \frac{4}{Re}\left[1 + 0.4Re^{1/2}{Sc_i}^{1/3} + 0.16Re^{1/2}{Sc_i}^{1/2}\right]$
Collection by interception	54	$E_{\Lambda intercept(i)} = 4\frac{r_i}{r_{rain}}\left[\frac{\mu_{air}}{\mu_{water}} + \left(1 + 2Re^{1/2}\frac{d_{ENP}}{d_{rain}}\right)\right]$
Collection by gravitational impaction	55	$E_{\Lambda grav(i)} = \left(\frac{St_i - St^*}{St_i - St^* + 2/3}\right)^{3/2} \quad if\ St_i > St^*$
Reynolds Number	56	$Re = \frac{d_{rain} \cdot v_{term(rain)} \cdot \rho_{air}}{2 \cdot \mu_{air}}$
Particle terminal velocity	57	$v_{term(i)} = \frac{{d_i}^2(\rho_i - \rho_{air})g \cdot Cc_i}{18\mu_{air}}$
Particle Schmidt Number	58	$Sc_i = \frac{\mu_{air}}{\rho_{air} \cdot D_{air(i)}}$
Particle Stokes Number	59	$St_i = \frac{2\tau_{air(i)}\left(v_{term(rain)} - v_{term(i)}\right)}{d_{rain}}$
Particle relaxation time	60	$\tau_{air(i)} = \frac{(\rho_i - \rho_{air}){d_i}^2 Cc_i}{18\mu_{air}}$
Critical Stokes Number (EΛgrav = o if St* > Sti)	61	$St^* = \frac{1.2 + \frac{1}{12}\ln(1 + Re)}{1 + \ln(1 + Re)}$

Table S17. Dry deposition velocities as a function of particle size and density.[5,7]

	Equation	
Dry deposition velocity of particle i to compartment 2	62	$v_{dep(i,dry\ air,2)} = \frac{1}{R_{A(2)} + R_{S(i,2)}} + v_{terminal(i)}$
Surface resistance	63	$R_{S(i,2)} = \frac{1}{u_*\left(E_{dBrown(i,2)} + E_{d\ int.cept(i,2)} + E_{dgrav(i,2)}\right)}$
Brownian collection at deposition to water	64	$E_{dBrown(i,water)} = {Sc_i}^{-1/2}$
Interception at deposition to water	65	$E_{d\ int.cept(i,water)} = 0$
Gravitational impaction at deposition to water	66	$E_{dgrav(i,water)} = 10^{-3St_i}$
Brownian collection at deposition to soil	67	$E_{dBrown(i,soil)} = {Sc_i}^{-2/3}$
Interception at deposition to soil	68	$E_{d\ int.cept(i,soil)} = \frac{Cv}{Cd}\left[fr_{iv}\left\{\frac{r_i}{r_i + \acute{a}_{veg}}\right\} + (1 - fr_{iv})\left\{\frac{r_i}{r_i + \acute{A}_{veg}}\right\}\right]$
Gravitational impaction at deposition to soil	69	$E_{dgrav(i,soil)} = \left(\frac{St_i}{St_i + \alpha_{veg}}\right)^{\beta_{veg}}$

Table S18. ENP dissolution rates*[1] for different mechanisms[3,24,25,38]

Mechanism	Equation	
Noyes-Whitney for readily soluble ENPs	70	$k_{dis(NW)} = A_{ENP}\frac{D_{SP}}{\delta_D}\left(\left[SP_{aq(0-\delta_D)}\right] - \left[SP_{bg}\right]\cdot M_{SP}\right)$
Practically insoluble	71	$k_{dis(I)} = 0$
Experimentally determined apparent dissolution rate	72	$k_{dis(exp.ment)} = -\frac{ln(C_0/C_{(t)})}{t}$
Dissolution following Arrhenius expression	73	$k_{dis(Arrhenius)} = c_{env.cond}\cdot A_{Arrhenius}\cdot e^{-E_{Activation}/RT}$

*1 The dissolution mechanism to be applied in SB4N is selected on the information that is available per case. Dissolution rates can also differ per aqueous medium and ENP species. SB4N easily deals with these possible differences, because its matrix A considers the environmental media as well as the free, aggregated, and attaches species of ENP. Different dissolution rates can be assigned per matrix cell and thus per environmental medium and ENP species.

Table S19. First-order rate constants for advective transports[14-16]

Mechanism	Equation	
Resuspension of free or agg ENPs	74	$k_{rsSEWfree,agg} = \frac{v_{rs}\cdot AREA_W}{VOLUME_{SE}}\cdot FR_{porewaterSE}$
Resuspension of att. ENPs	75	$k_{rsSEWatt} = \frac{v_{rs}\cdot AREA_W}{VOLUME_{SE}}\cdot FR_{solidsSE}$
Sediment burial	76	$k_{burSE(i)} = v_{bur}\cdot AREA_{SE}/VOLUME_W$
Pore water leaching of free or agg. ENPs	77	$k_{leachSfree,agg} = \frac{FR_{infiltration}\cdot p_0\cdot AREA_S}{VOLUME_{SOILPOREWATER}}$
Run-off of free or agg. ENPs	78	$k_{runSWfree,agg} = \frac{FR_{runsoil}\cdot p_0\cdot AREA_S}{VOLUME_{SOILPOREWATER}}$
Erosion of soil grains with ENPs attached	79	$k_{erosionSWatt} = \frac{v_{erosion}\cdot AREA_S}{VOLUME_{SOILSOLIDS}}$

Table S20. System dimensions for realistic nano-TiO_2 emission scenario in Switzerland[39]

Compartment	Area (m^2)	Height / depth (m)	Volume (m^3)
Atmosphere	$4.13\ 10^{10}$	1000	$4.13\ 10^{13}$
Soil*[1]	$4.00\ 10^{10}$	0.2*[2] and 0.05*[3]	$2.23\ 10^{9}$
Water	$1.24\ 10^{9}$	3	$3.7\ 10^{9}$

*1 Density of soil = 1500 kg. m^{-3}.[37] Soil is composed of a solid fraction of 0.6, a pore water fraction of 0.2 and an air fraction of 0.2[14-16]

Table S21. Input parameter and their values for the realistic nano-TiO_2 emission scenario in Switzerland[39]

Symbol	Parameter	Value
r_{ENP}	ENP radius	10 nm
ρ_{ENP}	ENP mass density	$4.23\ 10^{3}$ kg.m^{-3}
α_{agg}	Aggregation efficiency	0.1*[1]
α_{att}	Attachment efficiency	0.1*[1]
$k_{dissolve}$	Dissolution rate constant	0 s^{-1} *[2]

*1 Assumed default value

*2 No dissolution, as nano-TiO2 is practically insoluble.

Table S22. The first-order rate constant values that SimpleBox4nano calculates for environmental transport and removal processes for the Mueller and Nowack nano-TiO_2 emission scenario

Symbol	Transport / Removal Process	Rate*[1]
k_{aggA}	Aggregation rate for ENPs with aerosol particles in dry air (A)	1.57E-06 s^{-1}
k_{attA}	Attachment rate for ENPs with coarse particles in dry air (A)	1.32E-08 s^{-1}
$k_{\Lambda ARfree}$	Rain drop collection rate for free ENP species	6.02E-06 s^{-1}
$k_{\Lambda ARagg}$	Rain drop collection rate for aggregated ENP species	1.81E-06 s^{-1}
$k_{\Lambda ARatt}$	Rain drop collection rate for attached ENP species	4.44E-06 s^{-1}
$k_{depASfree}$	First-order rate constant for dry deposition from dry air (A) to soil (S) for free ENP species	1.59E-06 s^{-1}
$k_{depASagg}$	First-order rate constant for dry deposition from dry air (A) to soil (S) for aggregated ENP species	2.51E-07 s^{-1}
$k_{depASatt}$	First-order rate constant for dry deposition from dry air (A) to soil (S) for attached ENP species	9.41E-07 s^{-1}
$k_{depAWfree}$	First-order rate constant for dry deposition from dry air (A) to soil (W) for free ENP species	2.40E-08 s^{-1}
$k_{depAWagg}$	First-order rate constant for dry deposition from dry air (A) to water (W) for aggregated ENP species	2.80E-08 s^{-1}
$k_{depAWatt}$	First-order rate constant for dry deposition from dry air (A) to soil (W) for attached ENP species	3.00E-08 s^{-1}
$k_{depRSfree,agg,att}$	First-order rate constant for wet deposition from rain (R) to soil (S) for free, aggregated or attached ENP species	2.39E-03 s^{-1}
$k_{depRWfree,agg,att}$	First-order rate constant for wet deposition from rain (R) to water (W) for free, aggregated or attached ENP species	7.62E-05 s^{-1}
k_{aggS}	Aggregation rate for ENPs with natural colloids in soil (S) pore water	8.42E-07 s^{-1}
k_{attS}	Attachment rate for ENPs with solid grains in soil (S)	3.65E-03 s^{-1}
$k_{runSWfree,agg}$	First-order rate constant for run-off from soil (S) to water (W) for free or aggregated ENP species	2.93E-07 s^{-1}

$k_{erosionSWatt}$	First-order rate constant for run-off from soil (S) to water (W) for attached ENP species	1.68E-11 s^{-1}
$k_{leachSagg,free}$	First-order rate constant for run-off from soil (S) to water (W) for free ENP species	2.93E-07 s^{-1}
k_{aggW}	Aggregation rate for ENPs with natural colloids in surface water (W)	8.42E-07 s^{-1}
k_{attW}	Attachment rate for ENPs with suspended particles in surface water (W)	6.10E-10 s^{-1}
$k_{depWSEfree}$	First-order rate constant for deposition from water (W) to sediments (SE) for free ENP species	2.34E-10 s^{-1}
$k_{depWSEatt}$	First-order rate constant for deposition from water (W) to sediments (SE) for attached ENP species	2.36E-05 s^{-1}
$k_{depWSEagg}$	First-order rate constant for deposition from water (W) to sediments (SE) for aggregated ENP species	1.64E-08 s^{-1}
$k_{rsSEWfree,agg}$	First-order rate constant for resuspension from sediments (SE) to water (W) for free or aggregated ENP species*[2]	7.60E-07 s^{-1}
$k_{rsSEWatt}$	First-order rate constant for resuspension from sediments (SE) to water (W) for attached ENP species*[2]	3.04E-06 s^{-1}

*1 Calculated as a function of the system dimensions and default input parameters given in SI Table 16 and 17

*2 SB4N calculates the 1-year-PECs for this scenario as a function of one-directional transport only, since backward processes can usually be neglected. However, it should be considered that the backward resuspension process (an advective process that transports the free, aggregated, and attached ENPs that have settled in the sediment back to the water compartment) may not be negligible. Therefore, the influence of resuspension on both the 1-year-PECs in the water and sediment compartment has been investigated for this scenario. This was done by correcting the settling rates for backward resuspension by expressing resuspension as a resistance to settle:

$$v_{sett(netto,i)} = \frac{1}{1+\left({}^{v_{resusp}}/_{v_{sett(i)}}\right)} \cdot v_{sett(i)}$$

This approach has been verified by comparing the calculated concentrations PECs derived from the formulations for steady state, with the calculated concentrations using the corrected settling rates over infinite time. There were no major differences observed, which indicates that it is an acceptable approach to express resuspension as a resistance to settle for this scenario. However, this approach still neglects a minor mechanism contributing to concentration of ENPs attached to suspended particles in water: free ENPs may settle to the sediment and then attach to the solid grains in the sediment compartments. If these solid grains resuspend, they will transport these ENPs back the water compartment as attached species. Nonetheless, this mechanism actually can be assumed to be negligible as settling of free ENPs is negligible

compared to the settling behavior of ENPs attached to suspended particles, which is also observed in experiments[40]

AUTHOR INFORMATION

Corresponding Author

*Phone: +31-(0)24-3652393; e-mail : j.meesters@science.ru.nl

REFERENCES USED FOR SUPPORTING INFORMATION

(1) Van de Meent, D.; Hollander, A.; Peijnenburg; Breure, T. Fate and transport of contaminants. In *Ecological Impacts of Toxic Chemicals*; Sanchez-Bayo, F., van den Brink, P.J., Mann, R.M., Eds.; Bentham Science Publishers: 2011; pp 13-42

(2) Petosa, A.R.; Jaisi D.P.; Quevedo, I.R.; Elimelech, M.; Tufenkji, N. Aggregation and deposition of engineered nanomaterials in aquatic environments: Role of physicochemical interactions. *Environ. Sci. Technol.* **2010**, *44*, 6532–6549.

(3) Liu, J. Hurt, R.H. Ion Release Kinetics and Particle Persistence in Aqueous Nano-Silver Colloids. *Environ. Sci. Technol*. **2010**, *44,* 2169–2175

(4) Tufenkji N.; Elimelech M. Correlation equation for predicting single-collector efficiency in physicochemical filtration in saturated porous media. *Environ. Sci. Technol.* **2004**, *38*, 529–536.

(5) Nho-Kim, E.-Y.; Michou, M.; Peuch, V.-H. Parameterization of size-dependent particle dry deposition velocities for global modeling. *Atmos. Environ.* **2004**, *38,* 1933-1942

(6) Hinds, W.C.; *Aerosol Technology;* Wiley: New York, U.S. 1999.

(7) Kulmala, M; Dal Maso, J.; Makela, J.M.; Pirjola, J.; Vakeva, M.; Aalto, P.; Miikulainen, P.; Hameri, K.; O'Dowd, C.D. On the formation, growth and composition of nucleation mode particles. *Tellus* **2001**, *53B*, 479–490

(8) Jones E.H. ; Su, C. 2012. Fate and transport of elemental copper (Cu0) nanoparticles through saturated porous media in the presence of organic materials. *Water. Res.* **2012**, *46*, 2445–2456

(9) Ketzel, M.; Berkowicz, R. Modelling the fate of ultrafine particles from exhaust pipe to rural background: an analysis of time scales for dilution, coagulation and deposition. *Atmospheric Environment* **2004**, *38*, 2639–2652

(10) Tuteja A.; Mackay, M.E.; Narayanan, S.; Asokan, S.; Wong, M.S. Breakdown of the continuum stokes-einstein relation for nanoparticle diffusion. *Nanoletters*, **2007**, *7*, 1276–1281.

(11) Gong, S.L.; Barrie, L.A.; Blanchet, J.-P.; von Salzen, K. Lohmann, U.; Lesins, G.; Spacek, L.; Zhang, L.M.; Girard, E.; Lin, H.; Leaitch, R.; Leighton, H.; Chylek, P.; and Huang P. Canadian aerosol module: a size-segregated simulation of atmospheric aerosol processes for climate and air quality models: 1. module development. *J. Geophys. Res*. **2003**, *108* (D1), 3-16

(12) Gong, W.; Dastoor, A.P.; Bouchet, V.S.; Gong, S.L.; Makar, P.A.; Moran, M.D.; Pabla, B.; M´enard, S.; Crevier, L.-P.; Cousineau, S.; Venkatesh, S. Cloud processing of gases and aerosols in a regional air quality model (AURAMS), *Atmos. Res*. **2006**, *82*, 248–275

(13) Wang, X.; Zhang, L.; Moran, M.D. Uncertainty assessment of current size-resolved parameterizations for below-cloud particle scavenging by rain. *Atmos. Chem. Phys. Discuss.* **2010**, *10*, 2503–2548

(14) Van de Meent, D. *SimpleBox: a generic multimedia fate evaluation model. RIVM Report No. 222501002*; National Institute of Public Health and the Environment (RIVM): Bilthoven, The Netherlands, 1993.

(15) Brandes, L.J.; den Hollander, H.; van de Meent, D. *SimpleBox 2.0: a nested multimedia fat model for evaluating the environmental fat of chemicals. RIVM Report No. 670208001*; National Institute of Public Health and the Environment: Bilthoven, The Netherlands, 1996

(16) Den Hollander, H.; van de Meent D. *Model parameters and equations used in SimpleBox 3.0 RIVM Report No. 601200 003*; National Institute of Public Health and the Environment (RIVM): Bilthoven, The Netherlands, 2004

(17) Praetorius, A.; Scheringer, M.; Hungerbuhler, K. Development of Environmental Fate Models for Engineered Nanoparticles: A Case Study of TiO2 Nanoparticles in the Rhine River. *Environ. Sci. Technol*. **2012**, *46*, 6705−6713

(18) Brenner, H. The slow motion of a sphere through a viscous fluid towards a plane surface. *Chem. Eng. Sci*. **1961**, *16*, 241-251

(19) Hammes, J.; Gallego-Urrea, J.A.; Hasselov, M.2013. Geographically distributed classification of surface water chemical parameters influencing fate and behavior of nanoparticles and colloid facilitated contaminant transport *Water Res.* **2013**, *47*, 5350-5361

(20) Jaenicke, R.; *Aerosol Cloud-Climate Interaction*s; Academic Press Inc.: San Diego, U.S.., 1993.

(21) Quik, J.T.K.; Velzeboer, I.; Wouterse, M.; Koelmans, A.A.; van de Meent, D. Heteroaggregation and sedimentation rates for nanomaterials in natural waters. *Water Res.* **2014**, *48*, 269 – 279.

(22) Spielman, L.A.; Friedlander, S.K. 1974. Role of the electrical double layer in particle deposition by convective diffusion. *J. Colloid. Interface Sci.* **1974**, *46*, 22-31

(23) Van Jaarsveld , H. *The Operational Priority Substances model. Description and validation of OPS-Pro 4.1 RIVM report NO. 500045001/2004;* National Institute of Public Health and the Environment (RIVM): Bilthoven, The Netherlands, 2004

(24) Quik J.T.K.; Vonk J.A.; Hansen S.F.; Baun A.; van de Meent D. How to assess exposure of aquatic organisms to manufactured nanoparticles. *Environ. Int.* **2011**, *37*, 1068–1077.

(25) Godinez, I.G.; Darnault, C.J.G.; Khodadoust, A.P.; Bogdan, D. Deposition and release kinetics of nano-TiO2 in saturated porous media: Effects of solution ionic strength and surfactants. *Environ. Poll*. **2013**, *174*, 106-113

(26) Elimelech, M. Predicting collision efficiencies of colloidal particles in porous media. *Wat. Res*. **1992**, *26*, 1-8

(27) Seinfeld, J.H.; Pandis, S.N. *Atmospheric Chemistry and Physics: From Air Pollution to Climate Change;* John Wiley & Sons: New York, U.S., 2006.

(28) Gregory, J. Approximate Expressions for Retarded van der Waals Interaction. J. *Colloid. Interf. Sci.* **1981**, *83*, 138-145

(29) Putaud, J.P. ; van Dingenen, R.; Alastuey, A.; Bauer, H.; Birmilli, W.; Cyrys, J.; Flentje, H.; Fuzzi, S.; Gehrig, G.; Hansson, H.C.; Harrison, R.M.; Herrman, H.; Hitzenberger, R.;

Huglin, C.; Jones, A.M.; Kasper-Giebl, A.; Kiss, G.; Kousa, A.; Kuhlbusch, T.A.J.; Loschau, G.; Maenhaut, W.; Molnar, A.; Moreno, T.; Pekkanen, J.; Perrino, C.; Pitz, M.; Puxbaum, H.; Querol, X.; Rodriguez, S.; Salma, I.; Schwarz, J.; Smolik, J.; Schneider, J.; Spindler, G.; ten Brink, H.; Tursic, J.; Viana, M.; Wiedensohler, A.; Raes, F. A European aerosol phenomenology - 3: Physical and chemical characteristics of particulate matter from 60 rural, urban, and kerbside sites across Europe. *Atmos. Environ*. **2010**, *44*, 1308-1320

(30) Lyklema, H. *Fundamentals of interface and colloid science*; Elsevier Academic Press: Amsterdam, 2005

(31) Quik, J.T.K. Fate of nanoparticles in the aquatic environment, removal of engineered nanomaterials from the water phase under environmental conditions. Ph.D. Dissertation, Radboud University Nijmegen, The Netherlands, 2013.

(32) Keller, A.A.; Wang, H.; Zhou, D.; Lenihan, H.S.; Cherr, G.; Cardinale, B.J.; Miller, R.; Ji, Z. Stability and aggregation of metal oxide nanoparticles in natural aqueous matrices. *Environ. Sci. Technol.* **2010**, *44*, 1962-1967

(33) Everett; *Basic principles of colloid science*; The Royal Society of Chemistry: London, 1988.

(34) Elimelech, M.; Gregory, J.; Jia, X.; Williams, R.A.; *Particle Deposition and Aggregation: Measurement, Modeling, and Simulation*; Butterworth-Heinemann: Oxford, 1995.

(35) Zhang et al., Attachment Efficiency of Nanoparticle Aggregation in Aqueous Dispersions: Modeling and Experimental Validation. *Environ. Sci. Technol*. **2012**, *46*, 7054−7062.

(36) Struijs, J.; van de Meent, D.; Peijnenburg, W.J.G.M.; Heugens, E.; de Jong W.; Hagens, W.; de Heer, C.; Hofman, J.; Roex, E. *Nanoparticles in water;* National Insitute of Public Health and the Environment (RIVM): Bilthoven, The Netherlands, 2007

(37) Ruckenstein, E.; Prieve, D. C. Rate of deposition of Brownian particles under the action of London and double-layer forces. *J. Chem. Soc., Faraday Trans*. *2* **1973**, *69*, 1522–1536

(38) David C.A.; Galceran J.; Rey-Castro C.; Puy J.; Companys E.; Salvador J.; Monné J.; Wallace R.; Vakourov A. Dissolution kinetics and solubility of ZnO nanoparticles followed by AGNES. *J. Phys. Chem. C.* **2012**, *116*, 11758–11767.

(39) Mueller, N.C.; Nowack, B. 2008. Exposure Modeling of Engineered Nanoparticles in the Environment. *Environ. Sci. Technol.* **2008**, *42*, 4447–4453

(40) Quik, J.T.K.,; Stuart, M.C.; Wouterse, M.; Peijnenburg, W.; Hendriks, A.J.; van de Meent, D. Natural colloids are the dominant factor in the sedimentation of nanoparticles. *Environ. Toxicol. Chem.* **2012**, *31*, 1019-1022